Attitude Determination and Control System Design of the Hubble Space Telescope

Marco Hinojosa

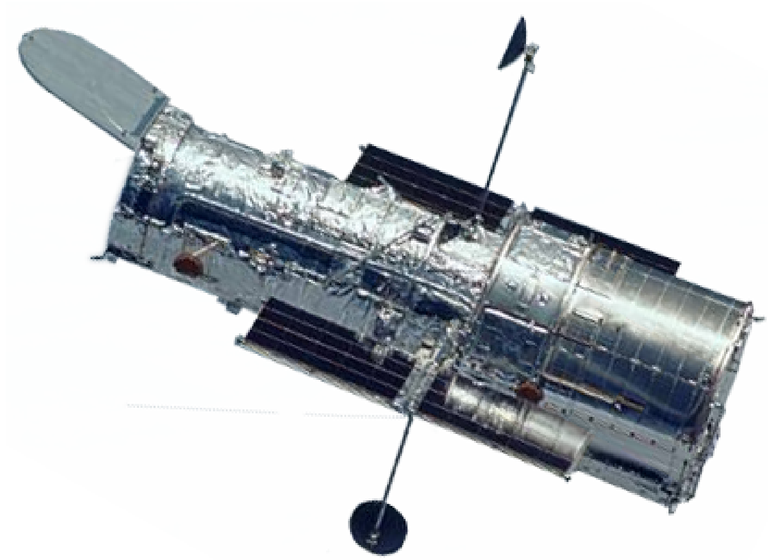

AA 279C - Spacecraft Attitude Determination and Control
Stanford University

GitHub: `https://github.com/marco-hinojosa/HST-ADCS`

Revision History

Table 1: Summary of project revisions.

Rev	**Changes**
PS1	- Created document - Added problem set 1 material
PS2	- Added problem set 2 material - Added rotation from body to principal axes
PS3	- Added problem set 3 material

Contents

1 Abstract

This report details the analysis of the attitude determination and control system (ADCS) design for the Hubble Space Telescope. This endeavor will encompass an understanding of the HST's mission objectives and target orbit, as well as the sensors and actuators present on the spacecraft and how they fulfill the requirements for the ADCS system. To Be Continued...

2 Mission Description and Requirements

The Hubble Space Telescope was designed as a direct solution to the problem of image distortion caused by the Earth's atmosphere. Since its launch in 1990, the HST has been fulfilling its mission of enabling astronomers to make extremely high resolution observations of deep space with considerably lower background light than ground-based telescopes. The Space Telescope Science Institute (STScI) at John Hopkins University has served as the science operations center for the HST, while Goddard Space Flight Center has been the control center for the spacecraft. The HST was built by NASA with contributions from the European Space Agency and has undergone five servicing missions since its initial launch. As of today, it has made over one million observations, some of which are the most detailed visible light images ever taken. The future of the HST's ongoing mission is largely dependent upon the extension of the telescope's service contract with NASA. If it is not reboosted, Hubble will undergo a natural atmospheric reentry at some time between 2028 and 2040.

The HST is an inertial-pointing satellite capable of taking images of distant, faint objects from low Earth orbit (LEO). Hubble has an altitude of approximately 540 kilometers and an inclination of 28.5^o that gives the spacecraft a period of approximately 95.5 minutes. The telescope is able to lock onto targets with an error no more than 7/1000th of an arcsecond and has a slew rate of approximately 6^o per minute [2]. To achieve this, Hubble must use three fine guidance sensors (FGSs) to receive highly accurate measurements of its attitude and then control it using four reaction wheels [3]. Along with star sensors and gyroscopes, Hubble also possesses gyroscopes, coarse sun sensors, magnetometers, and fixed head star trackers to determine its attitude to varying degrees of accuracy [5].

3 Spacecraft Model

A 3D CAD model of the Hubble Space Telescope was produced in SolidWorks, using known mass values and dimensions of the spacecraft [1]. This model was then used to determine the values in the Mass Properties table, assuming uniform density. The origin of the HST's body system was arbitrarily designated as the centroid of the bottom circular surface, according to the following figure. A simplified CAD model in which the satellite geometries were represented as boxes was used to determine centroids, normal vectors, and areas of each surface. This is a conservative approximation and simplifies calculations by reducing the total number of values to compute. Conveniently, these numbers are automatically computed in SolidWorks and are tabulated according to normal vector in Area Properties.

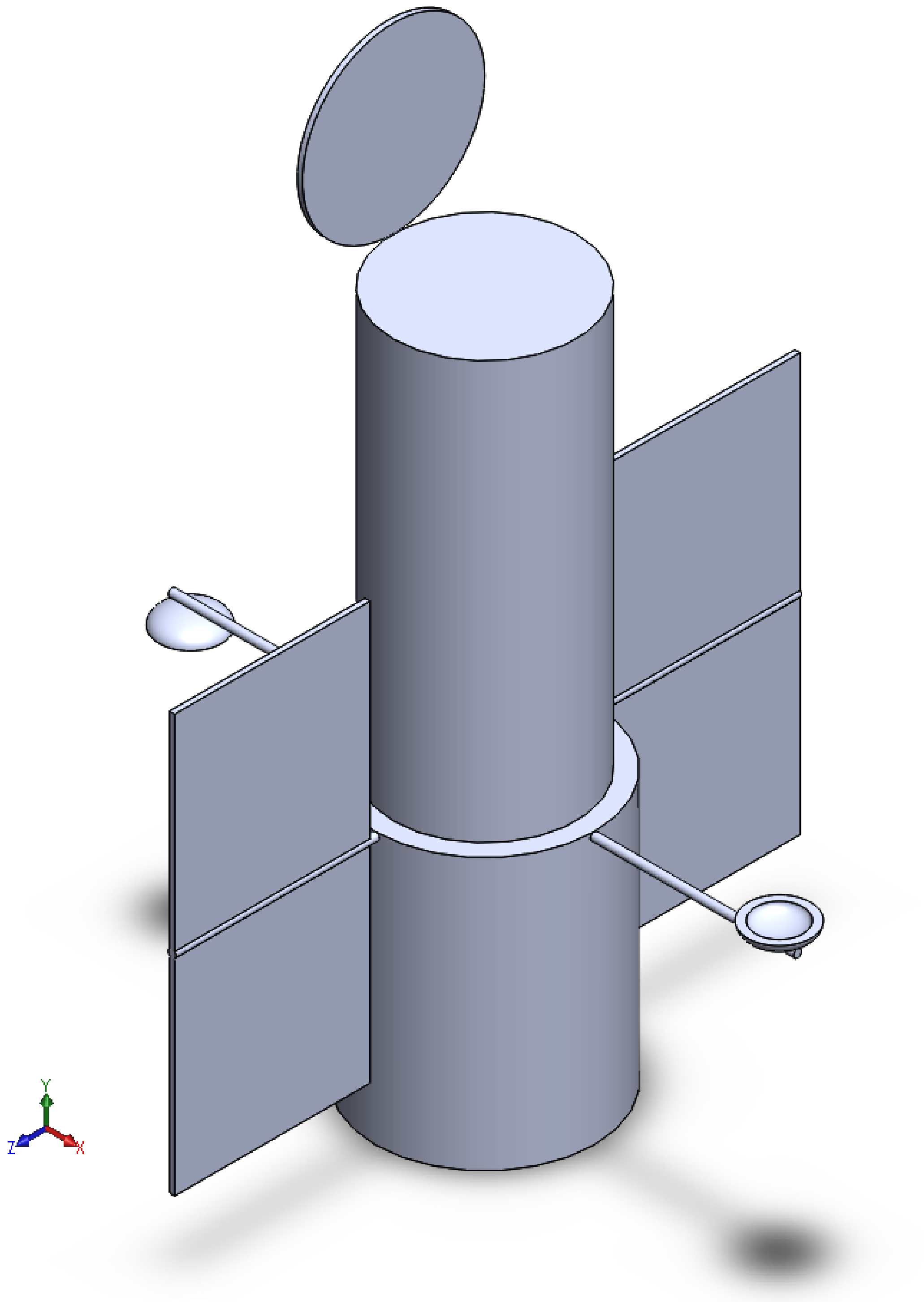

Figure 1: 3D CAD model of Hubble Space Telescope.

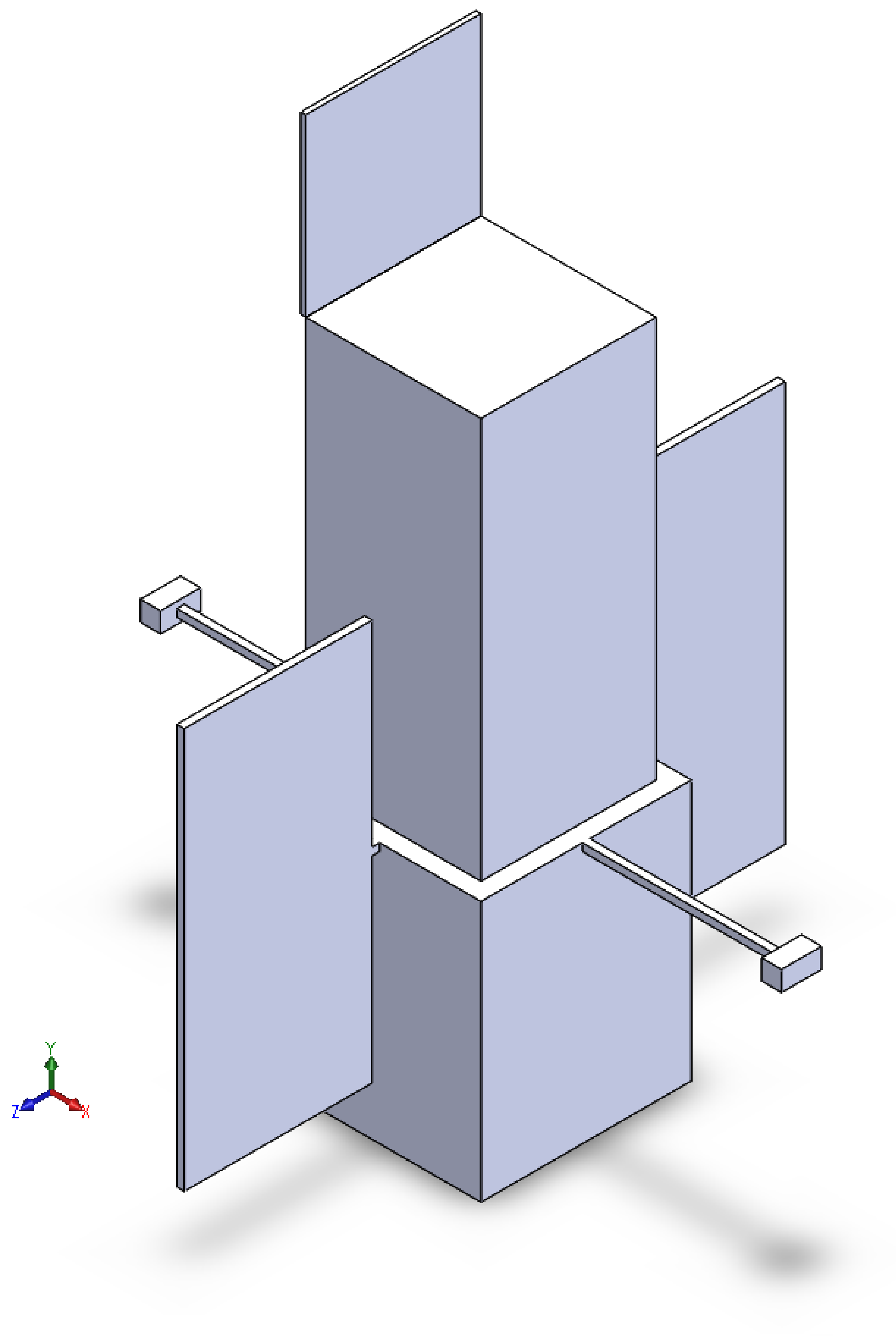

Figure 2: Simplified 3D CAD model of Hubble Space Telescope.

Mass Properties	
Mass (kg)	11,100
Volume (m^3)	156.43
Center of Mass (m) (w.r.t. Origin)	x = -0.01 y = 6.03 z = 0.00
Principal Axes of Inertia (Rotation Matrix from Body to Principal)	I_x = (-0.01, 0.00, -1.00) I_y = (-1.00, 0.00, 0.01) I_z = (0.00, 1.00, 0.00)
Principal Moments of Inertia (kg-m^2) (w.r.t. Center of Mass)	J_{11} = 28525.53 J_{22} = 174815.86 J_{33} = 181630.81
Body-Frame Inertia Matrix (kg-m^2)	${}^{B}\mathrm{J} = \begin{bmatrix} 181623.33 & -1070.20 & 0.00 \\ -1070.20 & 28533.02 & 0.00 \\ 0.00 & 0.00 & 174815.86 \end{bmatrix}$

Area Properties		
Normal Vector	Centroid (m) w.r.t. Origin	Area (m^2)
$\underline{n}$ = [1, 0, 0]	(x,y,z) = (0.64, 6.59, 0.00)	122.73
$\underline{n}$ = [-1, 0 ,0]	(x,y,z) = (-1.00, 6.59, 0.00)	122.73
$\underline{n}$ = [0, 1, 0]	(x,y,z) = (-0.03, 10.28, 0.00)	20.97
$\underline{n}$ = [0, -1, 0]	(x,y,z) = (-0.03, 0.72, 0.00)	20.97
$\underline{n}$ = [0, 0, 1]	(x,y,z) = (-0.01, 6.28, 1.85)	54.04
$\underline{n}$ = [0, 0, -1]	(x,y,z) = (-0.01, 6.28, -1.85)	54.04

From the tabulated information, the rotation matrix from body axes to principal axes is found to be

$$^{B}R^{P} = \begin{bmatrix} I_x \\ I_y \\ I_z \end{bmatrix} = \begin{bmatrix} -0.01 & 0.00 & -1.00 \\ -1.00 & 0.00 & 0.01 \\ 0.00 & 1.00 & 0.00 \end{bmatrix}$$

4 Dynamics

4.1 Keplerian Initial Conditions

The initial conditions of the simulation are provided as a set of Keplerian orbital elements and an initial epoch date and time. Orbital elements are available for this mission for several epoch times and can be used to replace the initial launch time.

All orbital elements are taken from Wikipedia.org at Epoch: 26 December 2017, 13:18:33 UTC [6].

$a = 6917.5$ km
$e = 0.000287$
$i = 28.47°$
$\Omega = 176.23°$

$\omega = 82.61°$
$M_0 = 319.41°$

4.2 Initial Position and Velocity in Inertial Frame

In order to numerically integrate our orbit equation, the initial Keplerian orbital elements must be converted to initial position and velocity vectors in an Earth-Centered Inertial (ECI) frame. Doing so gives the following vectors for the corresponding initial position and velocity in the appropriate ECI frame:

$r_0{}^{ECI} = [\,-5396.0,\ -3721.2,\ 2206.0\,]^T$ [km]
$v_0{}^{ECI} = [\,4.7443,\ -5.2827,\ 2.6893\,]^T$ [km/s]

4.3 Unperturbed Orbit Propagation

For an unperturbed system, vehicle dynamics behave according to the two-body problem, a simple second-order non-linear ODE expressed as

$$\ddot{\mathbf{r}} + \frac{\mu\mathbf{r}}{r^3} = \mathbf{0}$$

This ODE represents the gravitational acceleration acting upon the vehicle under ideal conditions (notably, the absence of other forces). Using the initial inertial states as provided in Section 4.2, the equation can be numerically integrated [7]. Neglecting all perturbation forces and gravitational forces from other bodies, the following orbit was integrated over a time spanning 3 complete orbits with a time step of 1 second.

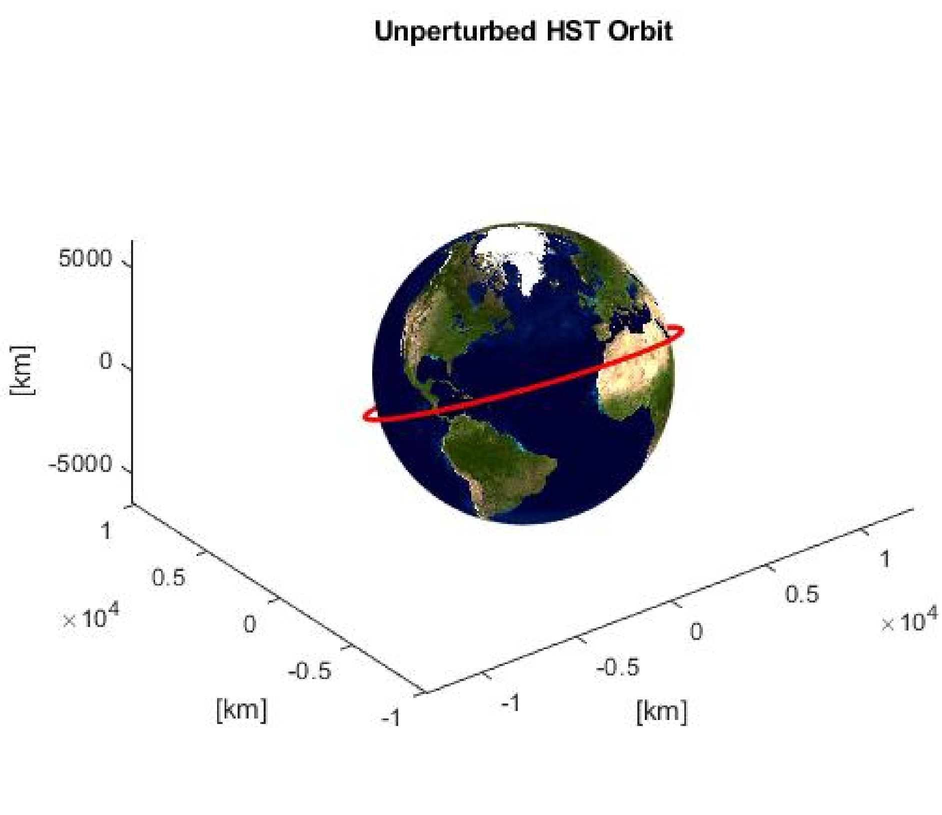

Figure 3: Unperturbed HST Orbit

4.4 Perturbed Spin Dynamics

The Gyrostat equation, a modified version of Euler's equation, must be implemented to examine the spin stability of the Hubble Space Telescope,

$$J\dot{\omega} + \dot{\rho} + \omega \times (J\omega + \rho) = \tau = 0$$

where J is the approximate inertia tensor from the simplified CAD model, ω is the angular velocity vector, and ρ is the rotor momentum for a gyrostat.The nominal spin of the HST can be visualized by setting $\rho = 0$ and simulating the dynamics the dynamics in MATLAB. The equilibrium points and nutation trajectories for various initial velocities are plotted on a momentum sphere in the following figure. All trajectories are subject to the constraint $\|J\omega\| = \|h\| = constant$.

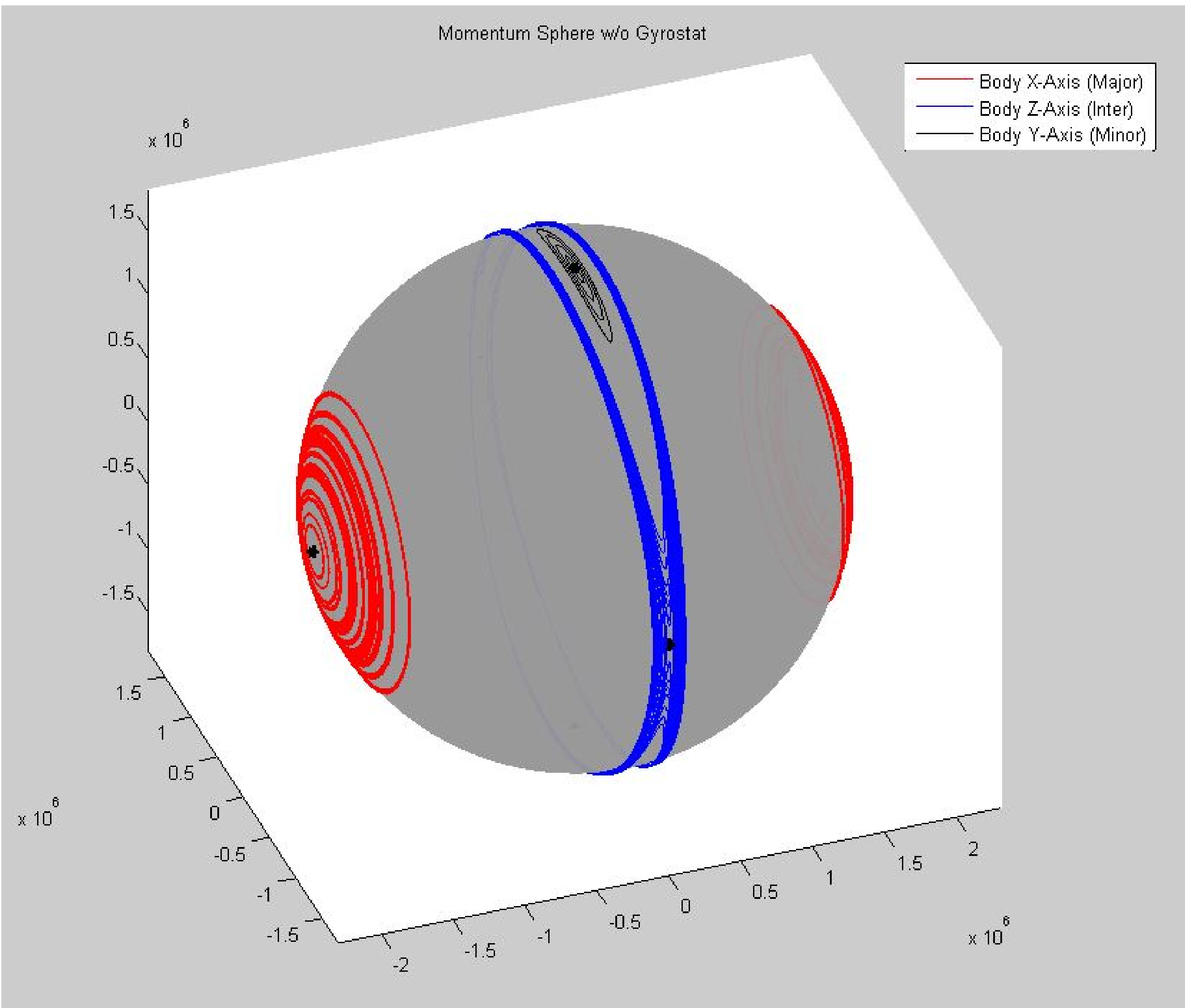

Figure 4: Perturbed HST Spin

4.5 Safe Mode

To implement a "safe mode" into the satellite design, we must use superspin and dynamic balance to stabilize the HST about a non-major axis. Based on the uniform-mass assumption of the CAD model created, the major axis corresponds to the x-axis in the body frame (rotation about this axis is a flat spin). For the sake of designing a safe mode, the body y-axis was arbitrarily selected to be the inertially fixed direction. To obtain the dynamic balance condition, the satellite and rotor must be in equilibrium, ${}^B\dot{\omega} = \dot{\rho} = 0$. For a nominal spin about this "effective major axis", the necessary rotor momentum can be computed from the equation

$$\rho = (J_{\text{eff}} - J_{33})\|\omega\|$$

where $J_{\text{eff}} = 1.2J_{33}$ for a conservative margin. Because we are assuming that there are zero external torques on the system, it is also safe to assume that $\dot{\rho} = 0$. Inserting these new values into the Gyrostat equation with small perturbations in the initial conditions results in the following nutation about the body y-axis. Visibly, the satellite is more tolerant of perturbations without moving into an unstable spin.

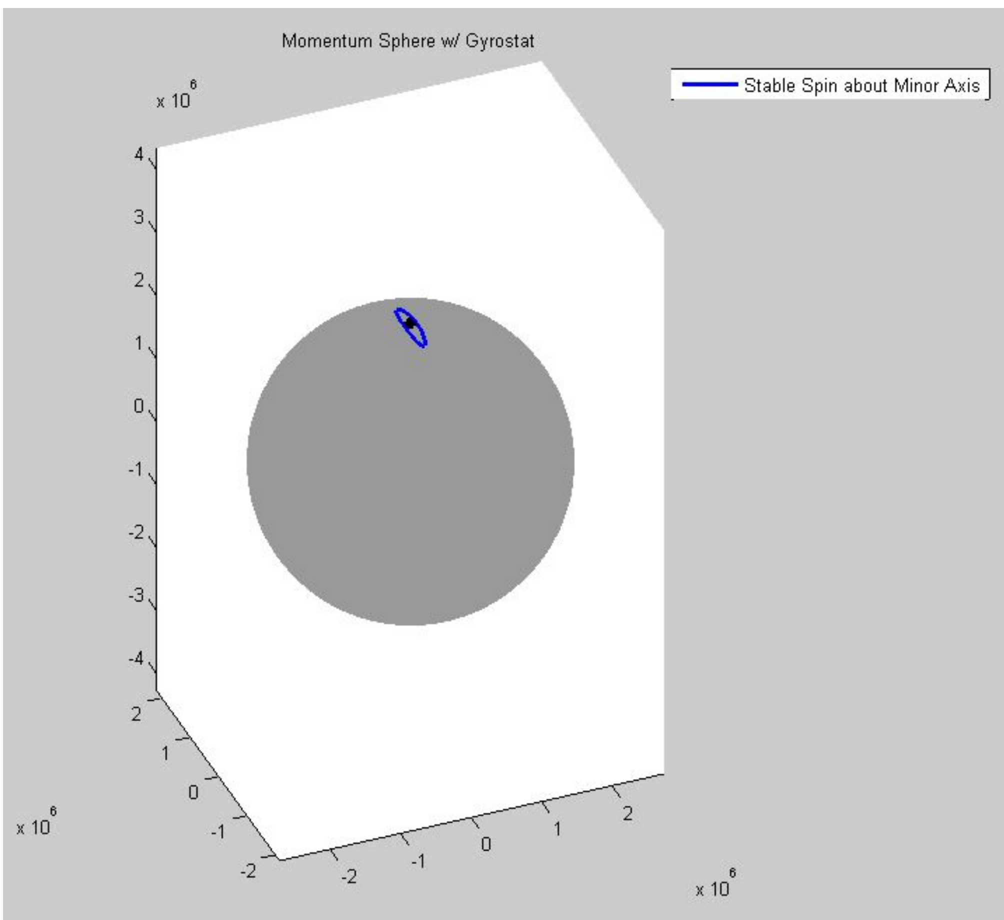

Figure 5: HST Spin about Non-Major Axis

4.6 Quaternion Dynamics

Simulating the gyrostat dynamics along with the orbit propagation is a simple matter of augmenting our existing state vector to include angular velocity, attitude quaternion, and rotor momentum and including the dynamics of each state element into our ODE solver. For the "safe mode" conditions, the components of the attitude quaternion of the HST are simulated and plotted over fifteen seconds in Figure 6.

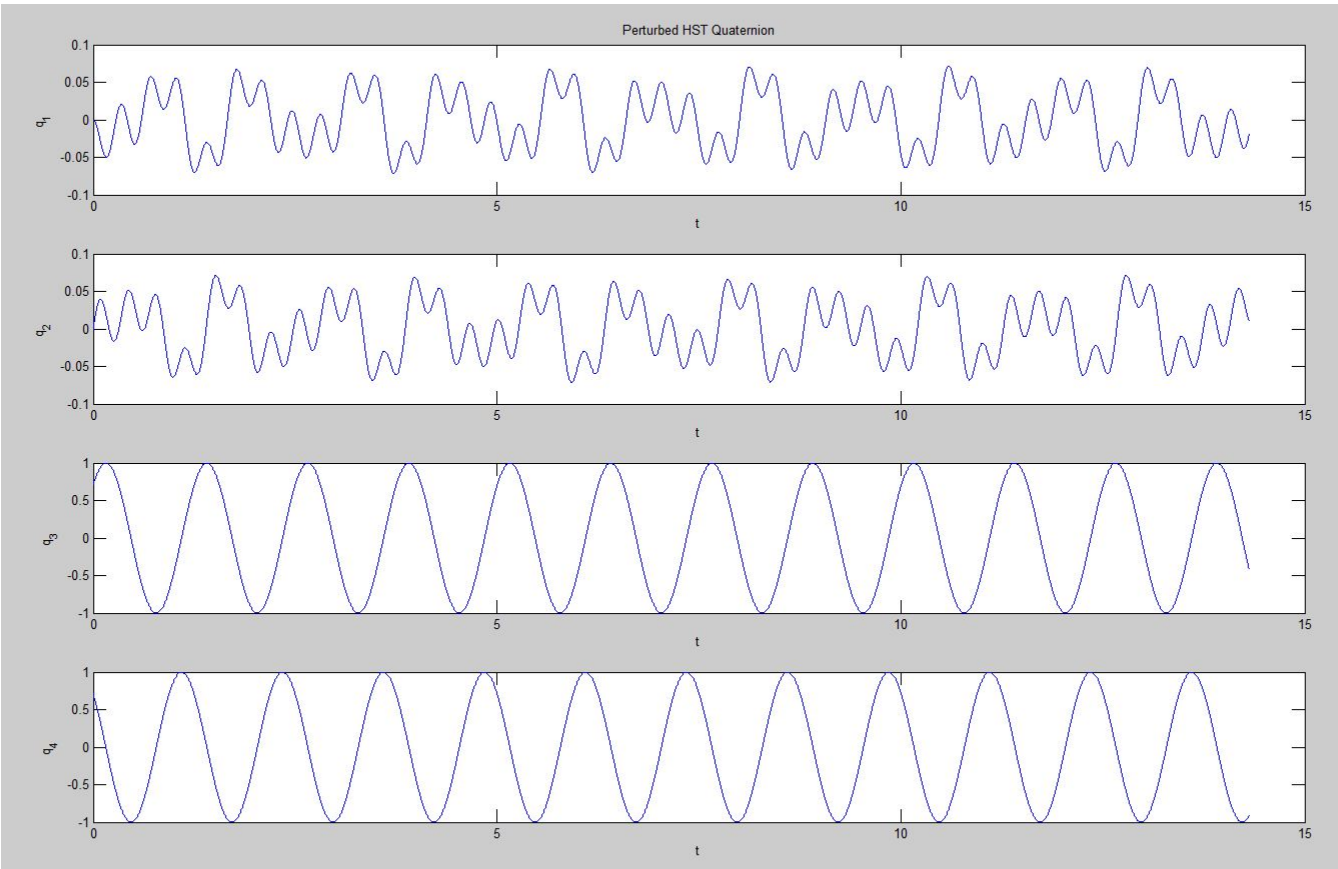

Figure 6: HST Quaternion

5 Attitude Sensors

The HST has five types of sensors that make up the Pointing Control System (PCS):

- Gyroscopes: Measures the telescope's 3-axis rotation rate in the satellite body frame. The gyros on the HST are some of the most accurate and stable ever built. However, the hardware inevitably degrades over time and creates measurement bias.
  - Rate Noise Density = 0.018 deg/s/sqrt(Hz).
  - Angular Random Walk = 0.002 deg/sqrt(hr).
- (Coarse) Sun Sensors: Determines the orientation of Hubble in relation to the Sun. The sensors use silicon diode detectors to determine whether the Sun is present in their field of view and the angle of the Sun relative to the sensor. This information is used to point the HST and protect the sensitive camera optics, which must be pointed at least 50^o away from the Sun at all times.
- Magnetometers: Measures the telescope's orientation in relation to Earth's magnetic field.
  - Magnetometer Error = 2 degrees or 0.035 radians.
- Star Trackers: Determines the HST's attitude by measuring the location and brightness of stars in the sensor's field of view. This information is then compared to star almanacs to increase the accuracy of the HST's attitude when locking onto guide stars.
  - Star Tracker Error = 36 arcseconds or 0.000174533 radians.
- Fine Guidance Sensors: Measures starlight captured by the telescope's mirrors to find and maintain a lock on guide stars to fix the satellite's attitude.
  - FGS Error = 2 milliarcseconds.

5.1 Static State Estimation

Static attitude state estimation is performed by solving Wahba's Problem, the least squares cost function

$$L = \sum_{\lim_i} w_i \left\| {}^N r_i - {}^N Q^{BB} r_i \right\|_2^2$$

whose optimal solution represents the minimum rotation matrix Q between an inertial reference frame and the body frame of a satellite. There are many solution techniques for this optimization problem, and the following figure contains a summary of error results for a Monte Carlo simulation consisting of $N = 2000$ trials using the TRIAD algorithm, the Davenport q-method, and the SVD method. To simplify the static calculations, the algorithms use one body-frame measurement from the magnetometer and a second body-frame measurement from an on-board GPS. As expected, the Davenport method and the SVD method provided nearly identical results with approximately 0.75 degrees of error, which is less than the 0.82 degrees of error from the TRIAD algorithm.

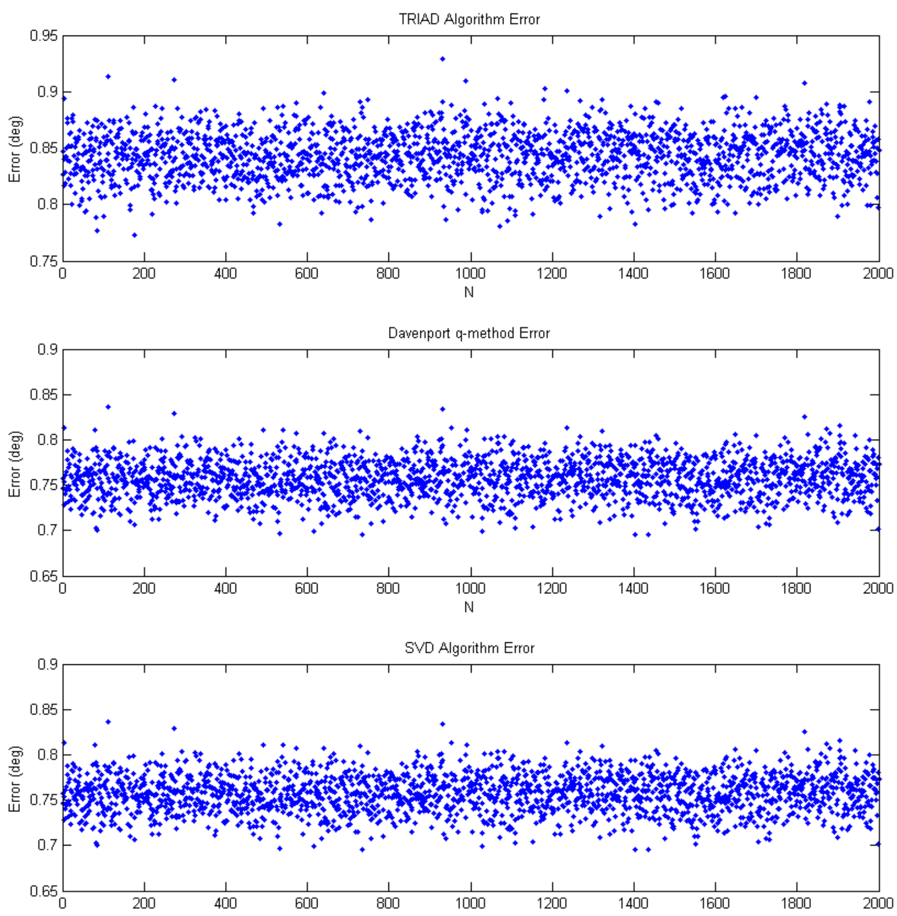

Figure 7: Monte Carlo Mean Error Results

The following subplots represent the static attitude state estimates over a time span of 5.75 seconds.

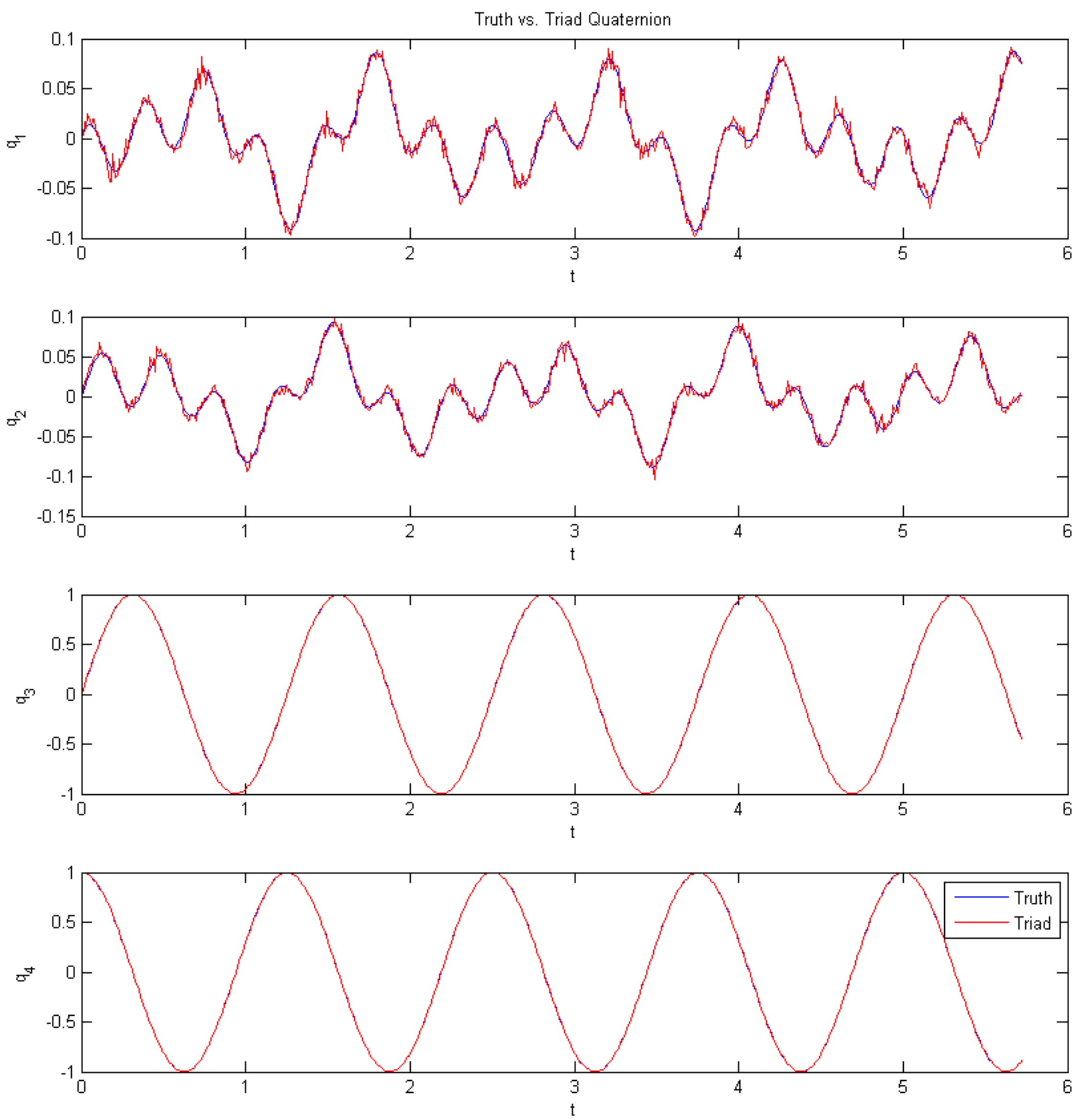

Figure 8: TRIAD Quaternion

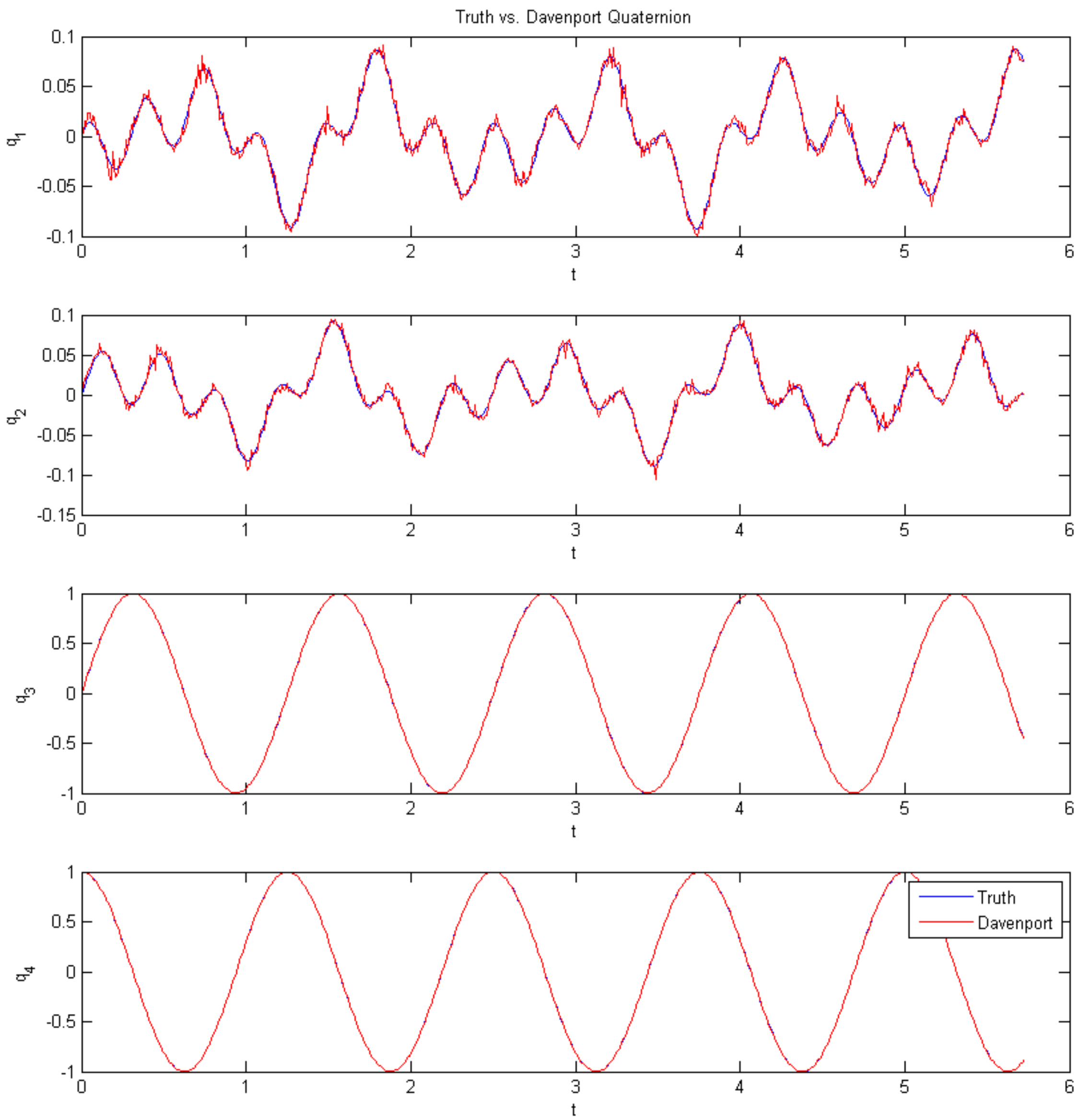

Figure 9: Davenport Quaternion

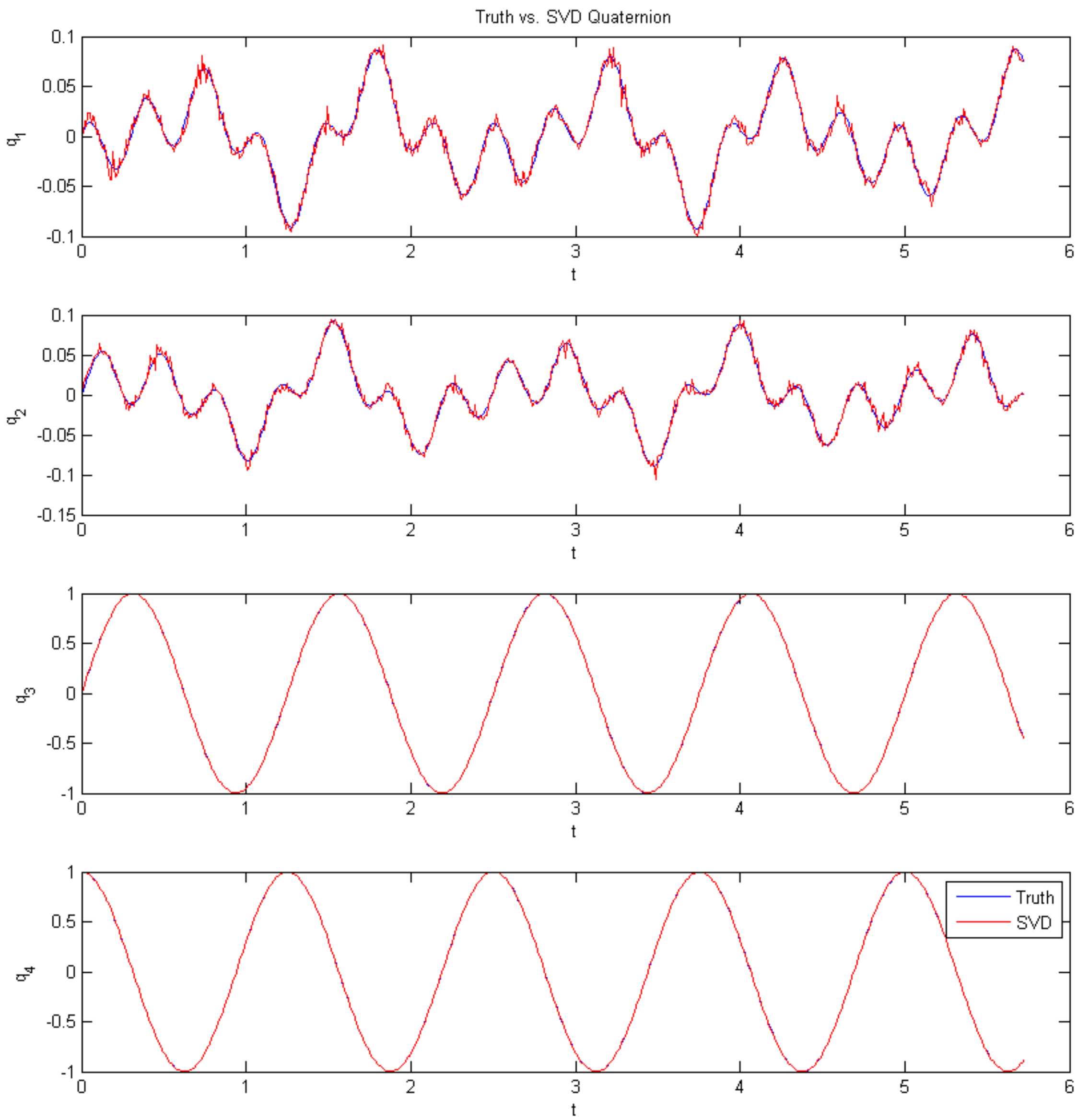

Figure 10: SVD Quaternion

5.2 Recursive Attitude Estimation

Using the simulated noisy measurements from the static state estimation, a Multiplicative Extended Kalman Filter can be implemented to recursively filter the sensor noise and estimate the gyroscope bias and spacecraft attitude with more accuracy than static methods. The MEKF function will eventually be modified to take in star tracker measurements.

Note: The MEKF does not properly track attitude error and gyro bias in its current state. More debugging is required.

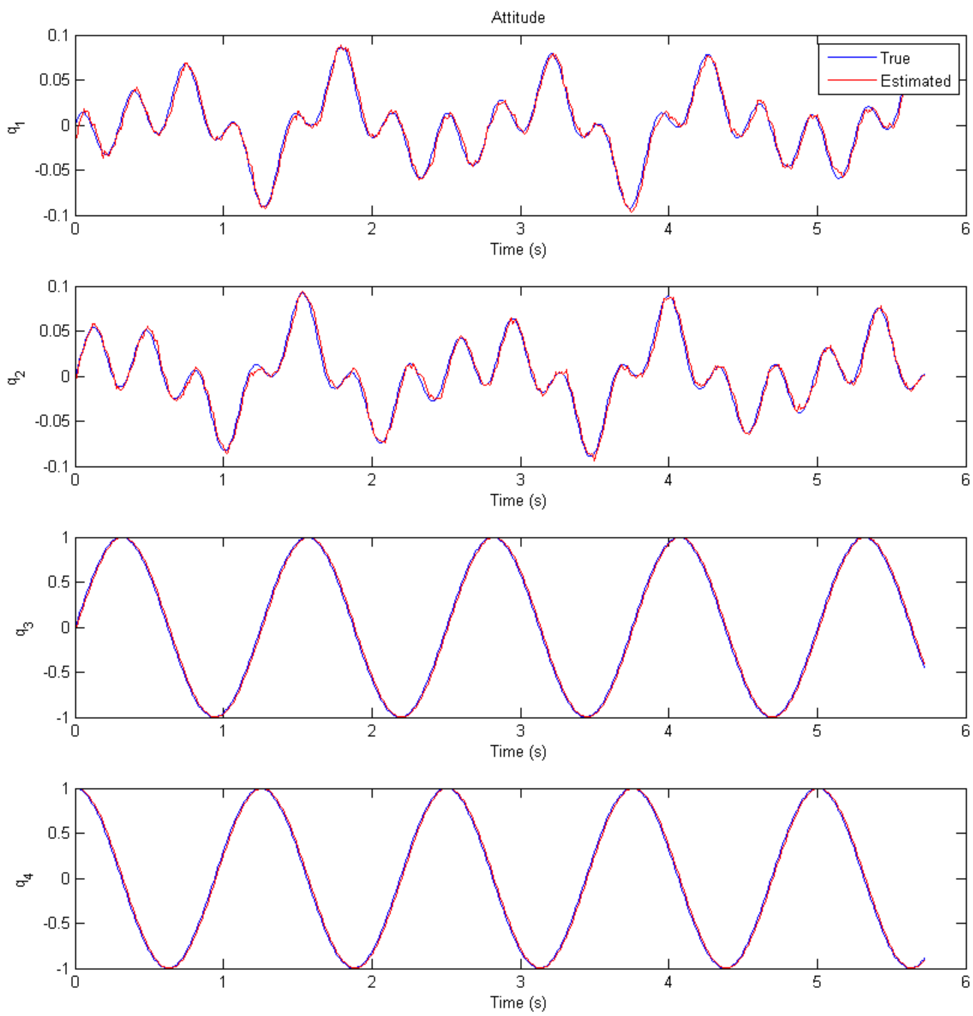

Figure 11: MEKF Attitude Estimate.

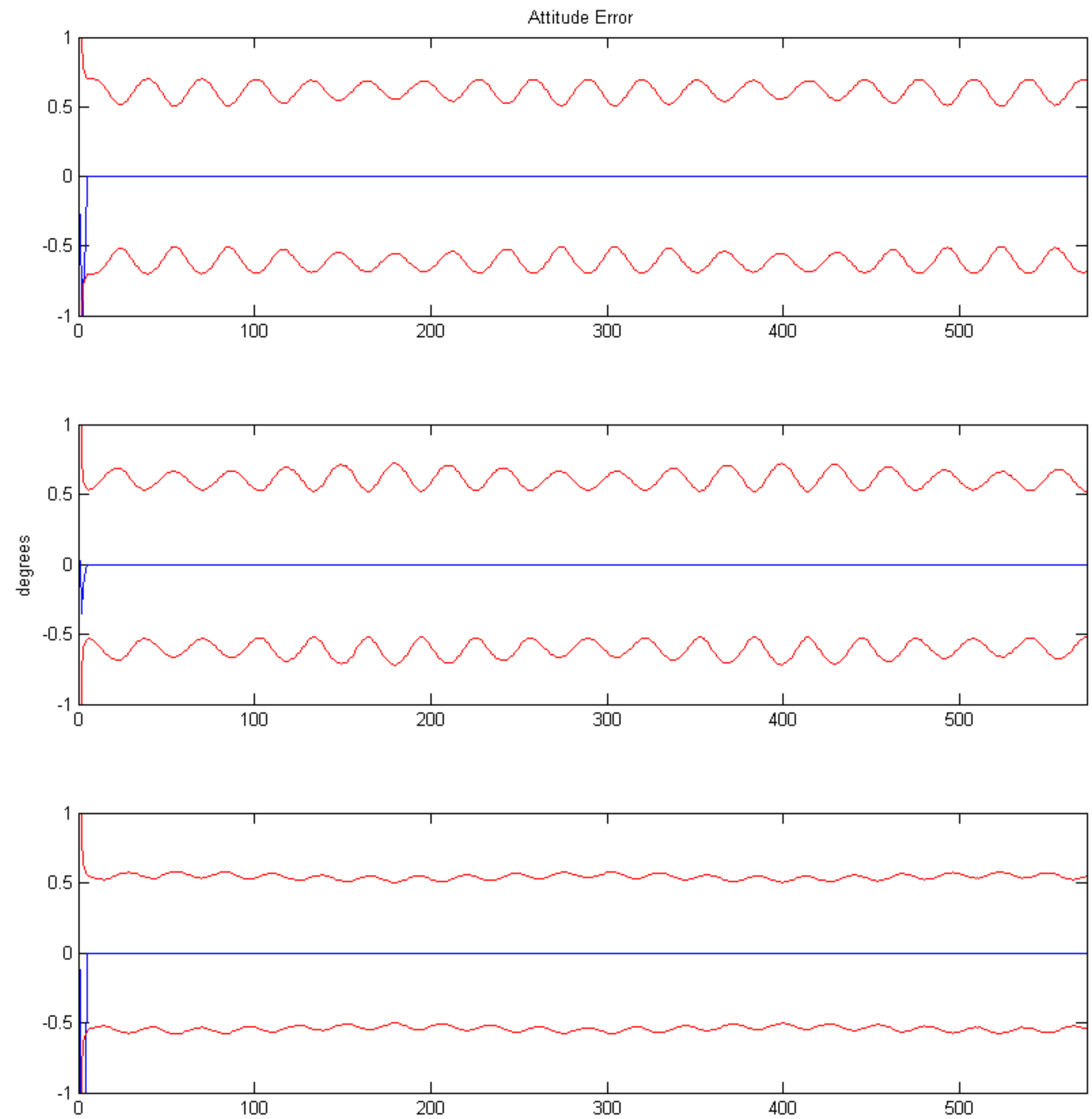

Figure 12: MEKF Attitude Estimate Error.

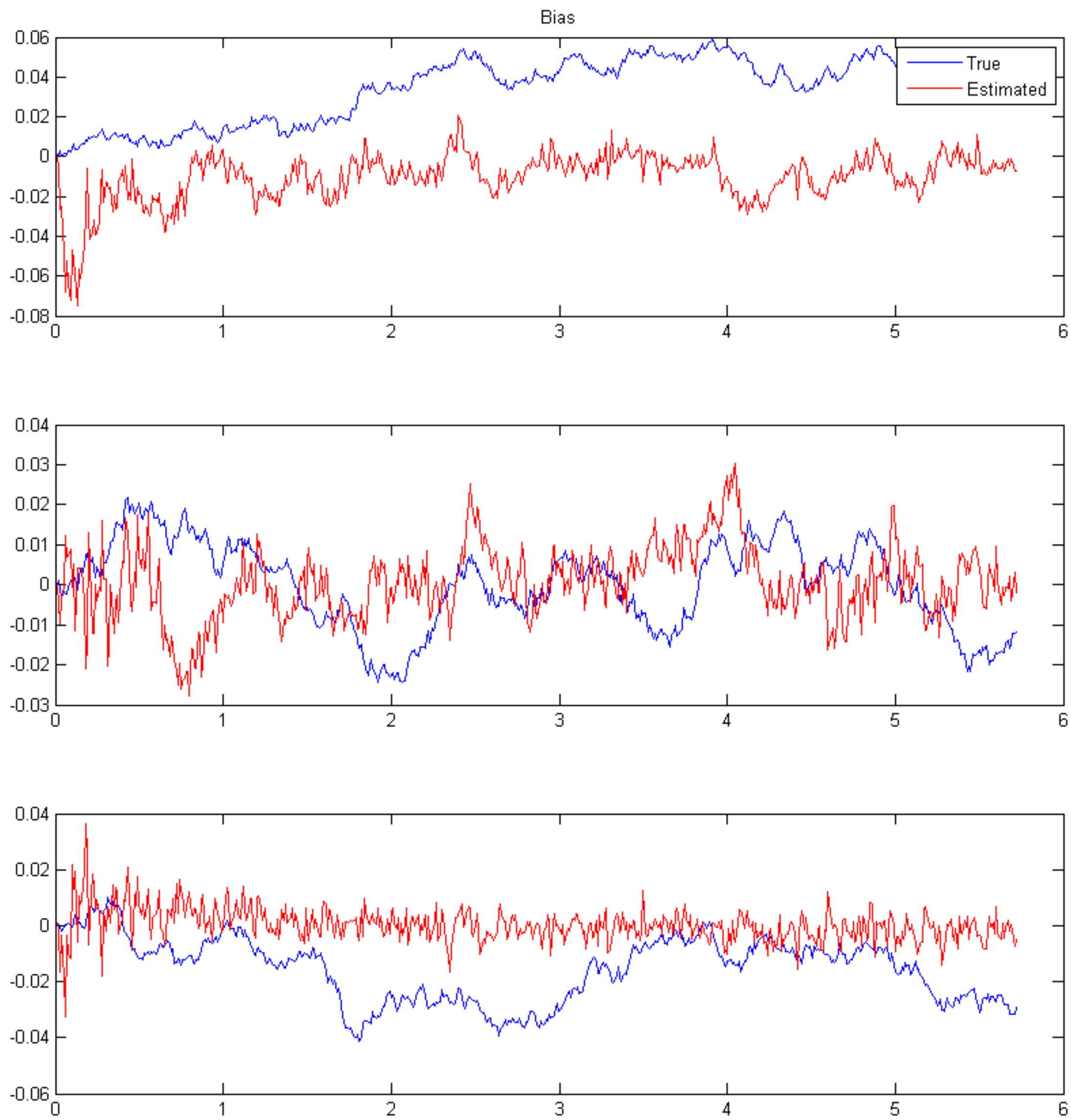

Figure 13: MEKF Bias Estimate

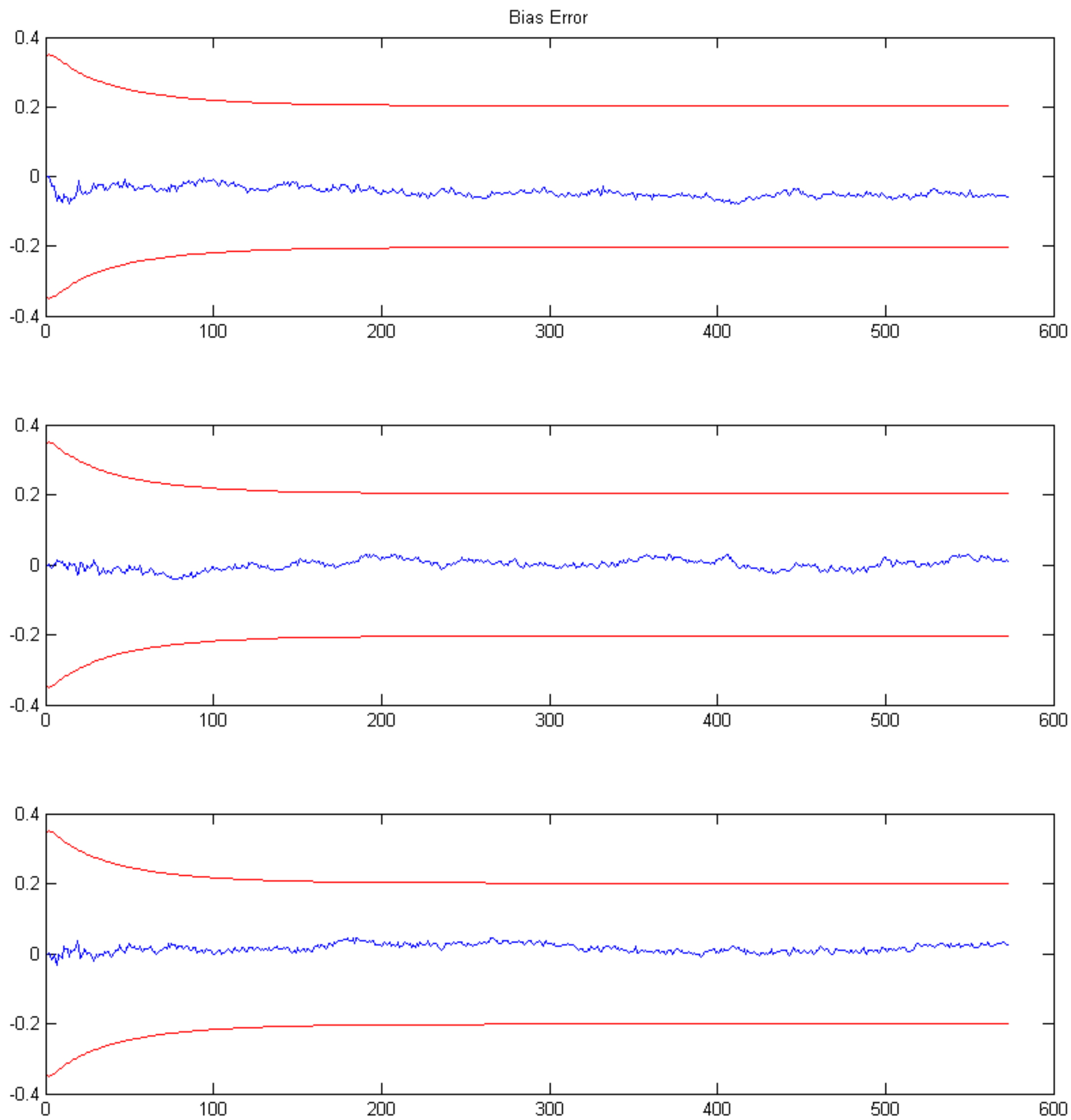

Figure 14: MEKF Bias Error.

References

[1] Hubble Space Telescope Fact Sheet. Retrieved April 24, 2018, from http://www.spacetelescope.org/about/general/fact_sheet/

[2] Hubble Space Telescope Primer for Cycle 25. Retrieved April 24, 2018, from http://www.stsci.edu/hst/proposing/documents/primer/primer.pdf

[3] The Telescope: Hubble Essentials. Retrieved April 24, 2018, from http://hubblesite.org/the_telescope/hubble_essentials/

[4] About the Hubble Space Telescope. Retrieved April 24, 2018, from https://www.nasa.gov/mission_pages/hubble/story/index.html

[5] Hubble Space Telescope Pointing Control System. Retrieved April 24, 2018, from https://www.nasa.gov/content/goddard/hubble-space-telescope-pointing-control-system

[6] Hubble Space Telescope. Retrieved April 24, 2018, from https://en.wikipedia.org/wiki/Hubble_Space_Telescope

[7] K. Alfriend, S. Vadali, P. Gurfil, J. How, and L. Breger, *Spacecraft Formation Flying: Dynamics, Control, and Navigation*. Elsevier Astrodynamics Series, 2010.